



A saliency-weighted orthogonal regression-based similarity measure for entropic graphs

Aslı Ergün¹ · Serkan Ergun² · Mehmet Zübeyir Ünlü³ · Cengiz Güngör²

Received: 14 June 2018 / Revised: 9 April 2019 / Accepted: 16 April 2019 / Published online: 4 May 2019
© Springer-Verlag London Ltd., part of Springer Nature 2019

Abstract

Various measures are used to determine similarity ratios among images before and after image registration. Image registration methods are based on finding the translation, rotation, and scaling parameters that maximize the similarity between two images by taking advantage of the feature points and densities that are found. While the similarity criterion is calculated, it is possible and advantageous to use approximation methods on the graphs based on information theory. The current study proposes a new similarity measure based on saliency-weighted orthogonal regression derived from the weighted sums of the saliency map of the orthogonal regression residuals formed on the entropic graph. It is evaluated in terms of both quantitative and qualitative methods and compared with other graph-based similarity measures.

Keywords Entropic graphs · Image registration · Parameter search / optimization technique · Feature sets · Joint saliency map · Orthogonal regression-based entropic graphs

1 Introduction

Image registration is the process of overlaying two or more images acquired at different times, at various view angles, and from different sensors on the same coordinate system. In medical image registration, the aim is to acquire more comprehensive and complementary information about a patient's condition and the status of their illness via the overlaid images [6].

Image registration benefits from the features and statistical density information of the images to be registered. When image registration is performed, the image, called *reference*

image, is kept steady, and the other, called *floating image* or *test image*, is deformed by applying the transformation. Similarity measures are used to measure the similarity of the reference and floating images before and after registration. Similarity measures take place in objective functions, and optimum transformation parameters are found when the dissimilarity value reaches the minimum.

Intensity-based similarity measures of images help to find the transformation parameter values where the pixel intensity is most similar with respect to pixel correlation. Probability-based similarity measures calculate the similarity values by determining the probability of occurrence of points in the image, probability ratios, and logarithmic distance of probabilities. According to these parameters, the similarity values are calculated and the most appropriate transformation is found. When probability-based similarity measures are calculated, approximation-based similarity values can be determined and used to reduce the cost of processing time and data size. One of the approximation methods is graph-based entropy method. Redmond and Yukich [18] have theoretically proven that similarity values computed via graph-based entropic measures overlap the formulated plug-in-based methods.

In image registration, the similarity measure between overlapping images is calculated to find the correct transform parameters. One of the most commonly used similarity mea-

✉ Aslı Ergün
asli.ergun@deu.edu.tr
Serkan Ergun
serkan.ergun@ege.edu.tr
Mehmet Zübeyir Ünlü
zubeyirunlu@iyte.edu.tr
Cengiz Güngör
cengiz.gungor@ege.edu.tr

¹ Department of Technical Programs, Izmir Vocational School, Dokuz Eylül University, Buca, Izmir, Turkey

² Ege University, Bornova, Izmir, Turkey

³ Electrical and Electronics Engineering Department, Izmir Institute of Technology, Urla, Izmir, Turkey

asures based on information theory is entropy, which measures the average knowledge between images and the predictability of information. The entropy measure can be calculated by observing the intensities of the pixel values of the point with plug-in formulas using the histogram values, or the graphical representation of the image in a joint histogram and formulation of its approximation.

Information theory-based image registration research began with Woods et al [25], who proposed a ratio-based criterion that indicates that the same type of brain tissue taken from different sources will coincide with the same point in images. Then, Hill et al [9] developed a new joint histogram-based measure by developing Woods' measure and then used a third-degree moment in the joint histogram showing the distribution inclination. Studholme et al [22] suggested that entropy could be used as a similarity measure in image registration. Collignon et al [4] and Viola and Wells III [23] stated that the concept of mutual information could be used in image registration. Mutual information similarity-based studies have been reviewed by Pluim et al [15]; Maes et al [13].

Redmond and Yukich [18] showed that the sum of the lengths of graph structures is asymptotically converged to a certain point and can be calculated with the help of certain coefficients. To obtain α -entropy similarity approximation, the sums of the Euclidean edges with coefficient weights are calculated. Examples of Euclidean graphs include *Minimum Spanning Tree (MST)* and *k-Nearest Neighbor (kNN)* graphs. Information theory similarity measures with the selected sample dataset can also use approximation methods. One of the entropy approximation methods is entropic graph-based structures, which is presented in the literature by several researchers such as [8,12,21]. They calculated the entropy by approximating the length of the graph-tree structure to the Renyi entropy formula.

Sabuncu and Ramadge [19] investigated entropic graphs using Delaunay triangulation. The MST graph generated from test and reference images was compared using the plug-in *Jensen–Renyi divergence (JRD)*. The application of gradient-based optimization registration was undertaken using the preliminary previously aligned image information. Bonev et al [2] developed methods of registration and classification using entropic graphs with maximum-saliency and minimum-error feature selection formulas. The graphs were calculated using the maximum-saliency and minimum-error joint saliency filters. Pál et al [14] showed that the sum of the Euclidean lengths of the edges of the kNN graphs could be approximated to Renyi entropy revealing the upper limits and continuity of the Renyi estimator.

Poczos et al [16] determined the Renyi entropy value using the copula distribution. Euclidean graph optimization was performed by ordering the edge weights, and as in filtering data using k-MST, a new similarity measure was

created using most significant graph edges. Sricharan et al [21] investigated the estimation of the Renyi entropy by creating weighted kNN graphs. The edge weights used were provided by convex hull optimization.

Qin et al [17] proposed the *joint saliency map (JSM)* method, in which unnecessary points were not processed, but images were overlaid with the help of mutual information similarity measure and more successful results were with less sensitivity to outliers. Zhang et al [26] used to create the MST graph and the Renyi entropy approximations by grouping corner and edge points features and for insufficient features assigning randomly feature values. Hazra et al [7] registered images according to the rotation angle and the regression line passing through the symmetric axis from the midpoints of objects. The regression analysis they used was based on spatial coordinates. Liu et al [10] proposed the use of saliency maps with *scale-invariant feature transform (SIFT)* points for feature selection. Singh and Poczos [20] used kNN graph statistics and designed a framework utilizing entropy and divergence for estimating nonparametric continuous probability distributions. Alam et al [1] proposed registration of images with the coefficients of curvelet transform using conditional entropy as the objective function.

In the current study, first, the SIFT features are minimized using the JSM method filters according to the importance of the points. Then, a new similarity measure is developed by creating a joint histogram on entropic graphs and summing the residuals of the regression line weighted by JSM. In addition, for the multimodal images, the images first are passed through the entropy filter; then, the similarity measure procedure is applied. This gives better results in terms of structural integration.

2 Entropic graphs and feature selection

Image registration is performed with the similarity measures obtained from graphs. Entropic graphs allow entropy estimation by using sampled points to connect to the edges to form a network structure based on the length of the graph. Entropic graphs are proximity graphs in which data point distances conform to a special geometric rule. There are many types of proximity graphs; Fig. 1 presents two types of entropic graphs.

Entropic graphs, compared to plug-in entropy approximation methods, approach asymptotic convergence limits faster, especially for features that do not have a smooth intensity transition and are less dimensional. This also decreases the cost of registration. Entropic graphs are created using the intensity values of the sampled points from reference and test images, and the length of the graph is approximated to entropy calculations. According to the similarity measure, the transformation parameter aligning the floating image to

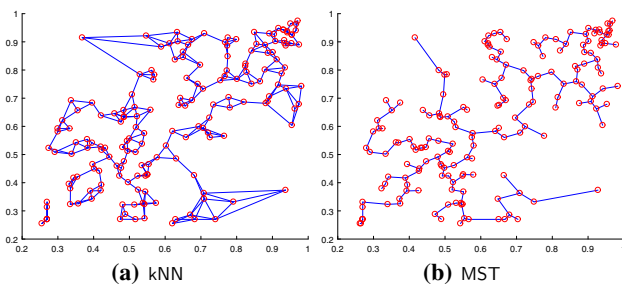


Fig. 1 Examples of entropic graphs

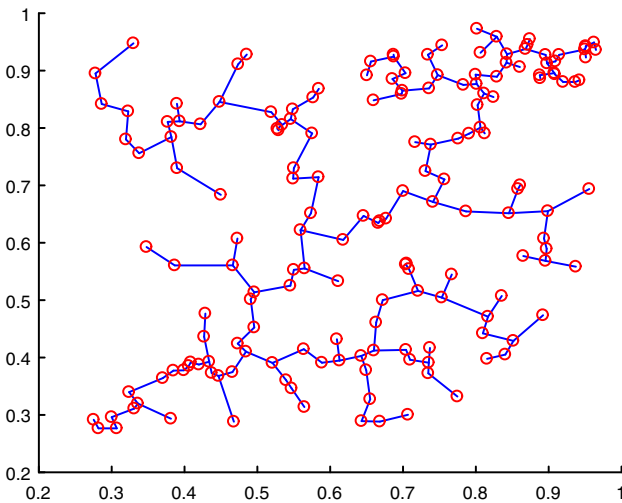


Fig. 2 MST graphs on a joint histogram

the reference image is calculated. In the entropic graph, one axis shows the intensity value of the reference image and the other axis shows that of the test image, ranging from 0 to 1 in floating numbers [8]. In both images, the same spatial coordinate values are found on the reference image and the intensity values of both reference and test images in the same spatial coordinate are plotted on the graph (Figure 2).

There is a relation between the proximity graph length and image entropy. This changes based on the graph type and similarity measure formulation. Redmond and Yukich [18] used the Lebesgue distance technique and took the MST length of asymptotic limit to determine the related parameters. From their results, Hero et al [8] approximated the MST length to the Renyi entropy as shown in equation (1).

$$H_{\alpha}(Z_n) = \frac{1}{1-\alpha} [\ln L(Z_n)/n^{\alpha} - \ln \beta_{L,Y}] \quad (1)$$

where Z_n , n is the point feature vector set, $L(Z_n) = \min \sum ||e||^{\gamma}$ refers to the total graph length of MST, $\beta_{L,Y}$, is the parameter calculated using the Lebesgue distance of MST asymptotic behavior, and α is the weight parameter and selected as $1/2$. The weight coefficient γ and entropy approx-

imation parameter α have a relation defined as $\alpha = \frac{d-\gamma}{d}$ and $\gamma = 1$ is selected.

Entropic graphs use feature points to connect the point via edges. In the current study, different groups of features were selected and compared, and these sample points were as follows: SIFT, *Speeded Up Robust Features (SURF)*, Harris corner, skeleton branch, and pyramid. SIFT algorithm returns a descriptor which is independent of scale and octave. SURF is a fast approximation of SIFT to find feature descriptors using integral image and box filter. SURF is better than SIFT in rotation invariant, blur, and warp transform. SIFT is better than SURF in different scale images. Because they are independent of the appearance of the images in the light conditions of the scene from which the scene is viewed without any approximations, the SIFT points were found to give a better feature representation of the entropic graphs [11].

3 Saliency-weighted orthogonal regression-based similarity measure

In this study, orthogonal regression entropy approximation on a joint histogram is applied and the sum of residuals to regression lines multiplied by the JSM weights is proposed as a new similarity measure.

3.1 Orthogonal regression on a joint histogram

Regression analysis is a method used to measure the relationship between two or more variables. Least square and total least squares (orthogonal regression) are data modeling techniques that reveal errors in the dependent and independent variables. They are the generalization of the multivariate Deming's regression [5] and can be applied to linear and non-linear models. Unlike the linear regression method, it takes into account errors in both x and y directions (Figure 3).

In the experiments, when transformation parameters obtained by the optimization approach are the optimum solution, the entropic graphs are condensed on the regression line (Fig. 4).

In a similar way, when orthogonal regression measure is applied, the residuals are condensed on the regression line and the sum of the residuals becomes minimum when the transformation parameters align with the reference and floating images (Fig. 5).

Both the entropic graph length and orthogonal regression residual sums are proportional to the data point size on normal, uniform, and triangular distributions (Fig. 6).

The results related to the MST and orthogonal regression graphs raise the issue of the relation between the Renyi entropy and the sum of the orthogonal regression residuals. In order to show this relationship, both the MST length and

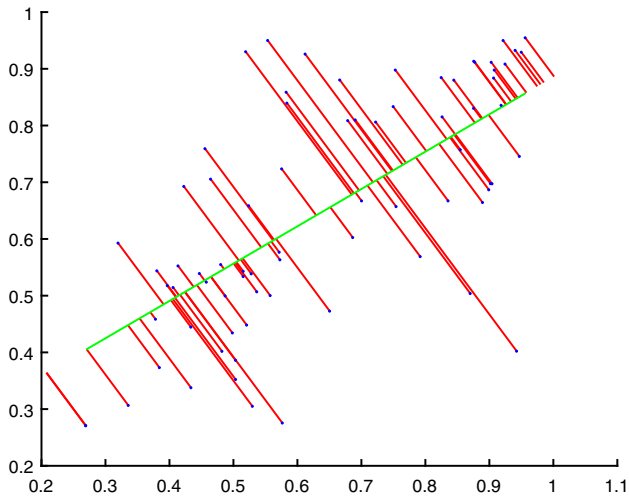


Fig. 3 Orthogonal regression line and residual graphs

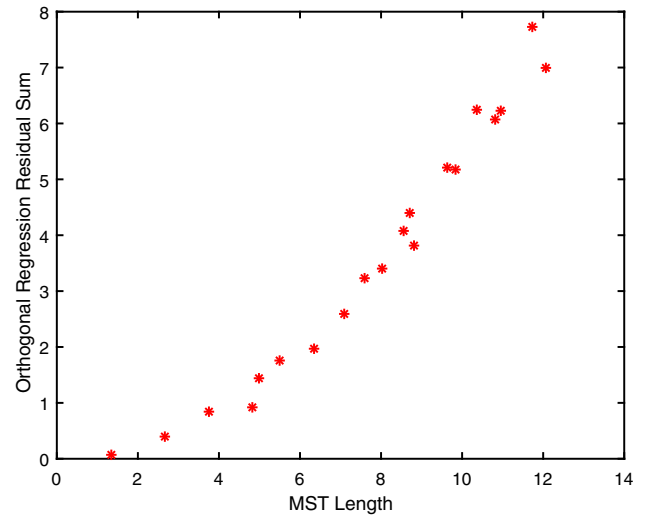


Fig. 7 MST graph and orthogonal regression ratios

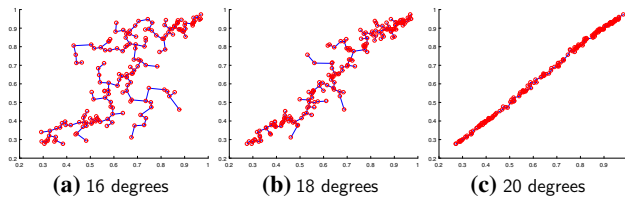


Fig. 4 MST graph characteristics on the regression line. The reference image is rotated 20° to obtain the floating image. MST entropic graphs are as presented when the floating image is rotated by given degrees

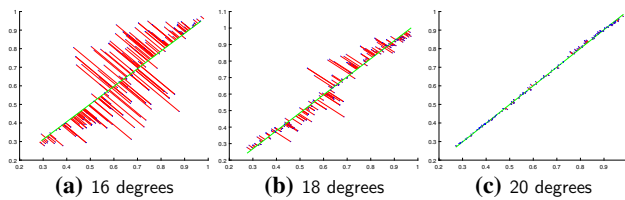


Fig. 5 Orthogonal regression residual characteristics on the regression line. The reference image is rotated 20° to obtain the floating image. Entropic orthogonal regression graphs are as presented when the floating image is rotated by given degrees

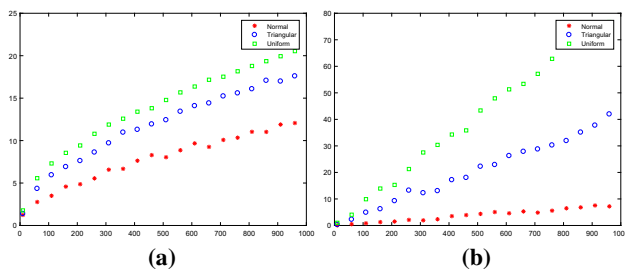


Fig. 6 Data size and graph length ratios of **a** MST and **b** orthogonal regression residuals

orthogonal regression residual for uniform distribution are plotted and observed the logarithmic linear ratio (Fig. 7).

The SIFT feature points are selected, and then, JSM filter is applied to shrink the feature point set. JSM was used both in the feature selection and for similarity measure weight calculations. For the multimodal images, after preprocessing and finding the region of the interest, entropy filter was applied. Image entropies are used for structural image representations and the images are filtered with the entropy filter. In this process, each of the pixel neighborhood windows is defined and the entropy of the center pixel is calculated. Multimodal images can be brought to the same structural base and their similarities can be calculated for image registration [24]. Figure 8 presents a flowchart of this process.

3.2 Joint saliency map (JSM)

JSM was first proposed by Qin et al [17], who created saliency structures on a weighted joint histogram. With the use of joint saliency maps on feature selections in cases where badly overlaid images such as deformation on floating images and tumor appearances in illness cases, sensitivity during registration decreases and better results are obtained in calculating mutual information and entropy measures. JSM values change between 0 and 1, and the overlapping salient pairs give the highest values.

In the creation of JSM, first, the contrast adjustments saliency operator $S_l(v)$ is applied to 1 pixel neighborhood of the region. In equation (2), the (u, v) points are neighborhood points, to which the operator is applied.

$$S_l(v) = \sum_{u \in N_v} (I_l(v) - I_l(u))^2 \tag{2}$$

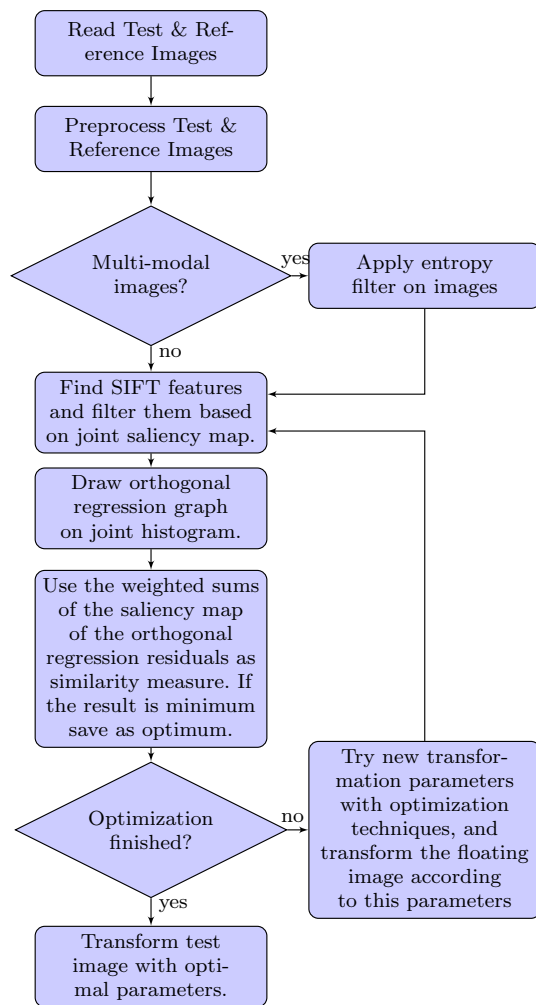


Fig. 8 Flowchart of the saliency-weighted orthogonal regression-based similarity measure

$S_l(v)$ is the local saliency computed for the intensity $I_l(v)$ in the Gaussian image pyramid at scale l and $I_l(u)$ is the intensity of the pixel in the $I_l(v)$'s neighborhood.

Then, on different Gauss image pyramids, the saliency vector is applied to perform the same procedure and the results added all together. *Principal axis analysis (PAA)* is applied, and the most important axes are chosen for the first eigenvalue pair for the *regional saliency vector (RSV)*. The saliency vector dot products of both the reference and floating images are used as JSM.

In the current study, first, the SIFT features were selected, and the JSM was applied as a filter. In this process, the selected features were decreased by 30% so that the selected landmark points were more meaningful for the similarity measure calculations. The selected feature points are applied to the new similarity measure using JSM weights to find the best overlaid positions of the reference and floating image for registration.

Table 1 Optimization results comparisons for MST similarity measure and pyramid feature points

Method	X	Y	θ	RMSE	Elapsed time (sec)
Simplex	-4.51	-5.38	-4.99	2.94	72.78
Steep. D.	-4.39	-5.05	-4.97	3.80	20.03
Conj. G.	0.02	0.01	0.01	8.48	18.44

4 Experimental results

In this work, entropic graph-based similarity measures and the proposed saliency-weighted orthogonal regression-based similarity measure were compared to demonstrate the performance advantages of the proposed method. All the experiments were performed on brain images and rigid registrations. The images used in the experiments were taken from BrainWeb [3] and other open-source databases from the Internet. Images from BrainWeb are T1- and T2-weighted *magnetic resonance (MR)* images with 3% noise and 20% non-uniformity, and in the dimensions of $217 \times 181 \times 181$. All the datasets were used as sliced magnetic resonance (MR) images.

Image registration experiments are undertaken in three main categories: feature sets, similarity measure sets (entropic graph and orthogonal regression based), and optimization sets. In the experiments, for the same modalities, floating images were deformed by a 5° rotation (θ) and transforming the reference images by 5 pixels (X,Y). In the first experiment, different images were experimented to test the performance of saliency-weighted orthogonal regression-based similarity with saliency map filtered SIFT feature points and steepest descent optimization. In this experiment, the saliency-weighted orthogonal regression-based similarity gave the best result. Since orthogonal regression was undertaken within an entropic joint histogram domain, saliency-weighted orthogonal regression-based similarity can be considered as an entropic graph measure.

Table 1 shows the results of the MST similarity measure and pyramid feature points according to three different optimization techniques by taking previous research as a reference. According to these results, the steepest descent algorithm shown in the second row of the table gives the best overall results. Figure 9 presents the images corresponding to the data given in Table 1. In Fig. 9, the first column represents the *reference image*, the second column represents the *test image*, and third to fifth columns represent *resulting images after simplex, steepest D. and conjugate G. optimization methods*, respectively. The difference of the reference and corresponding images is shown in the second row.

Table 2 shows the results of the MST similarity measure and steepest descent optimization comparing different feature selections, and Fig. 10 presents the related images. The

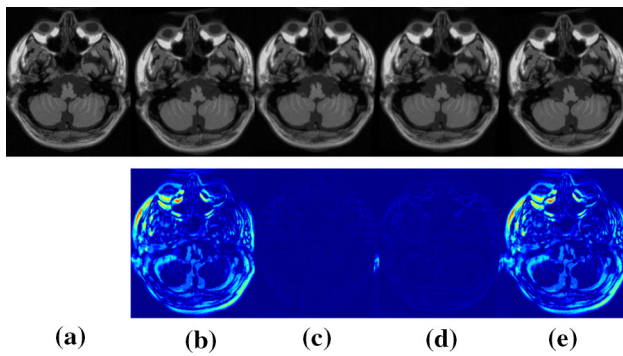


Fig. 9 Images for the comparison of optimization results. **a** Original image. **b** Test image **c–e** shows the images registered using simplex, steepest D., and conjugate G. algorithms, respectively. The bottom row shows the differences with the original image

Table 2 Comparison of different selected features using MST similarity measure and steepest descent optimization

Method	X	Y	θ	RMSE	Elapsed time (sec)
SIFT	-4.65	-5.52	-4.93	3.12	13.64
SURF	-2.40	-2.07	0.61	8.09	10.13
Harris	-0.03	-1.28	0.95	8.46	12.99
Skeleton	-4.39	-5.35	-4.94	3.17	17.90
Pyramid	-4.39	-5.05	-4.97	3.80	20.07

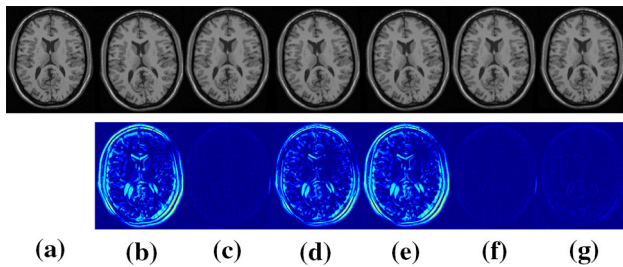


Fig. 10 Images for the comparison of the results based on the selected features. **a** Original image. **b** Test Image **c–e** shows the images registered using SIFT, SURF, Harris, skeleton, and pyramid feature points, respectively. The bottom row shows the differences with the original image

best result was obtained from the SIFT with saliency map filter feature. The columns in the figure represent the *reference image*, *floating image*, *aligned image*, *the difference between the reference and floating image*, and *the difference between the reference and the aligned image*, respectively.

Table 3 and Figure 11 present the reference and test images registered using the SIFT points with saliency map filtered features, steepest descent optimization, and entropic similarity measures. The best result is obtained with saliency-weighted orthogonal regression-based similarity measure.

Table 4 and Figure 12 give the results on the T1-weighted and T2-weighted MR images registered using the SIFT points with saliency map filtered features, steepest descent

Table 3 Comparison of the different applied similarity measures using SIFT points with saliency map filtered features and steepest descent optimization

Method	X	Y	θ	RMSE	Elapsed time (sec)
MST	-4.48	-5.65	-5.05	3.32	13.75
Orth. Regr.	-4.71	-5.42	-4.97	3.18	26.55
Sal. W. Orth. Regr.	-4.47	-5.56	-4.95	3.13	27.38
kNN	-1.85	-6.11	-17.76	8.47	14.24
Gabriel	0.04	0.03	-0.06	8.55	11.55

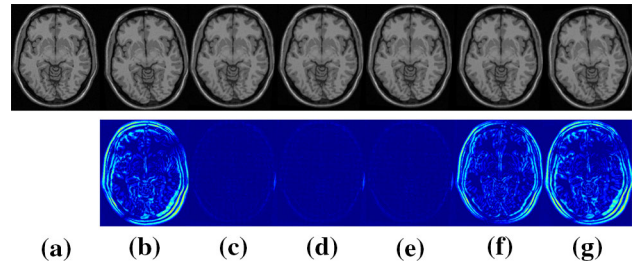


Fig. 11 Images for the comparison of the results based on similarity measures. **a** Original image. **b** Test Image **c–g** shows the images registered using MST, orthogonal regression saliency feature, orthogonal regression saliency weighted, kNN, and Gabriel, respectively. The bottom row shows the differences with the original image

Table 4 Similarity measure comparison of the T1–T2 Multimodal image results using SIFT points with saliency map filtered features and steepest descent optimization

Method	X	Y	θ	MI	Elapsed time (sec)
Sal. W.	-3.98	-4.26	-4.61	1.022	25.31
MST	0.18	-0.44	-0.00	1.001	12.36
kNN	-0.67	1.27	1.48	1.001	15.24

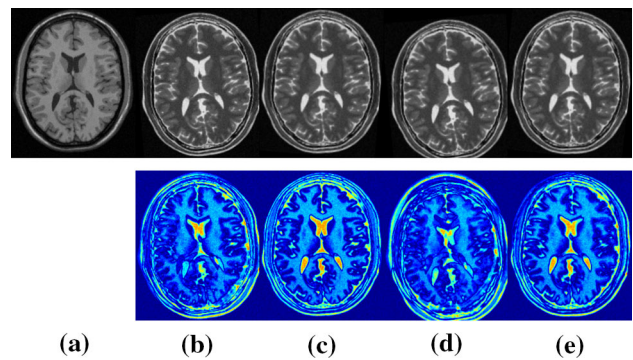
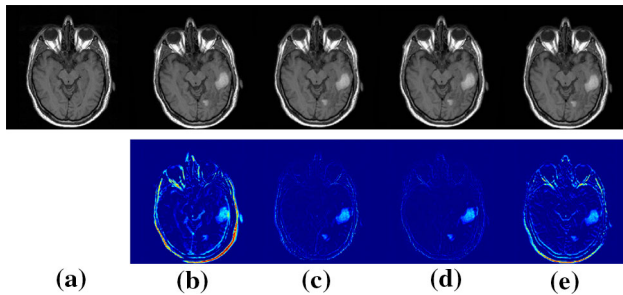


Fig. 12 Multimodal (T1–T2) images presenting the results of the saliency-weighted orthogonal regression-based similarity measure comparison for the SIFT features and the steepest descent optimization. **a** T1 image. **b** T2 image **c–e** shows the images registered using orthogonal regression saliency weighted, MST, and kNN. The bottom row shows the differences with the original image

Table 5 Similarity measure results for images with or without brain tumor using SIFT points with saliency map filtered features and steepest descent optimization

Method	X	Y	θ	RMSE	Elapsed time (sec)
Sal. W.	-4.49	-4.46	-5.12	4.09	56.36
MST	-5.00	-4.85	-5.47	4.70	21.95
kNN	-2.99	-0.10	-5.09	6.39	29.24

**Fig. 13** Disease-free T1 and T1 with tumor images presenting the results of the saliency-weighted orthogonal regression-based similarity measure comparison for the SIFT features and steepest descent optimization. **a** Disease-free T1 image. **b** T1 with tumor. **c–e** shows the images registered using orthogonal regression saliency weighted, MST, and kNN. Bottom row shows the differences with the original image**Table 6** Comparison of similarity measures for multimodal images with and without MS disease using SIFT features with saliency map filtered features and steepest descent optimization

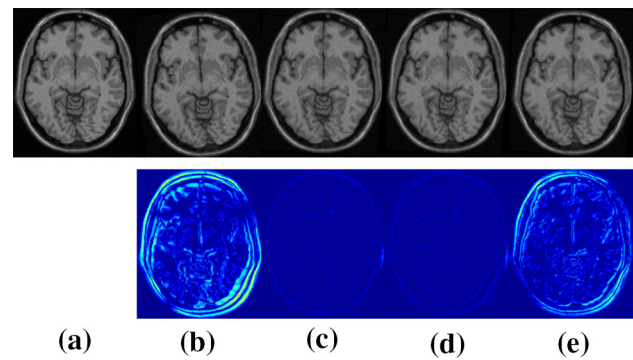
Method	X	Y	θ	RMSE	Elapsed time (sec)
Sal. W.	-6.38	-5.99	-4.05	7.60	26.87
MST	-2.68	-0.89	-13.24	9.20	16.61
kNN	-0.07	7.61	-13.64	9.42	17.05

optimization, and saliency-weighted orthogonal regression-based similarity measure.

Table 5 and Figure 13 show the results on the disease-free T1 and T1 with tumor images registered using the SIFT points with the saliency map filtered features, steepest descent optimization, and the saliency-weighted orthogonal regression-based similarity measure has given the best result.

Table 6 and Figure 14 show the results of T1 and T1 with *multiple sclerosis (MS)* images registered using the SIFT points with saliency map filtered features, steepest descent optimization and saliency-weighted orthogonal regression-based similarity measure with MS images obtained from the BrainWeb database [3].

Table 7 and Figure 15 present the results of the saliency-weighted orthogonal regression-based similarity measure based on different transformation start degrees of registration using SIFT points with saliency map filtered features and the steepest descent optimization.

**Fig. 14** A set of T1 and T1 with MS images presenting the results of the saliency-weighted orthogonal regression-based similarity measure comparison for the SIFT features and steepest descent optimization. **a** Disease-free T1 image. **b** T1 with MS **c–e** shows the images registered using orthogonal regression saliency weighted, MST, and kNN. The bottom row shows the differences with the original image**Table 7** Registration results for different start transformation degrees for the rotated floating image

Initial degree	X	Y	θ	RMSE
5	0.07	-0.19	-5.07	3.09
10	0.00	-0.19	-10.08	3.16
15	4.51	0.73	-0.31	8.78
20	0.12	-0.07	-19.96	3.22
25	0.05	-0.11	-25.11	3.30

5 Conclusions

In this study, a saliency-weighted orthogonal regression-based similarity measure was proposed. Feature selection and transformation parameter optimization techniques were compared using a graph structure. In the experimental studies, the SIFT points with saliency map filtered features were the fewest and the best descriptors of the images and saliency-weighted orthogonal regression-based similarity measure gave better results compared to other entropic graphs.

As a similarity measure, the saliency-weighted orthogonal regression provided better results than the other entropic graph-based similarity measures. The mathematical relation between the orthogonal regression residual sum and the Renyi entropy formula was empirically shown. In future work, the coefficients have to be found in the conversion equation of the orthogonal regression residual sum and the Renyi entropy. In this way, entropy values can easily be calculated with regression errors.

The proposed saliency-weighted orthogonal regression-based similarity measure gave better results in different images including the multimodal and unimodal images. In

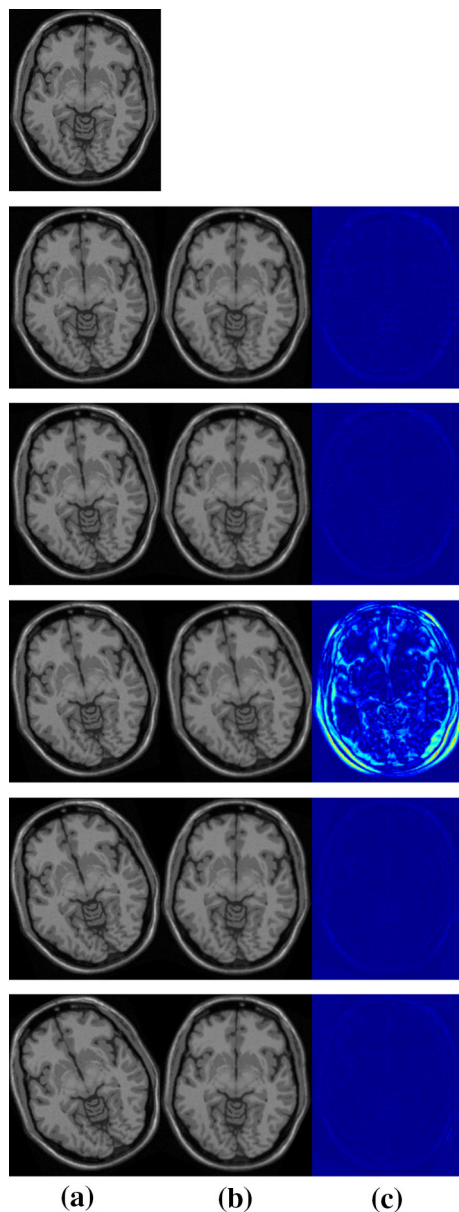


Fig. 15 Images presenting the results of the saliency-weighted orthogonal regression-based similarity measure based on different transformation start degrees of registration using SIFT feature and steepest descent optimization. **a** Test image. **b** Reconstructed image **c** image differences. The first row is the original image, and 2nd – 6th rows are rotated 5, 11, 15, 20, and 25°, respectively

the future, different images of various diseases can be registered and various datasets can be created to support the diagnosis of different conditions.

References

- Alam, M., Howlader, T., Rahman, S.M.M.: Entropy-based image registration method using the curvelet transform. *SIVIP* **8**, 491 (2014). <https://doi.org/10.1007/s11760-012-0394-1>
- Bonev, B., Escolano, F., Cazorla, M.: Feature selection, mutual information, and the classification of high-dimensional patterns. *Pattern Anal. Appl.* **11**(3), 309–319 (2008). <https://doi.org/10.1007/s10044-008-0107-0>
- Cocosco, C.A., Kollokian, V., Kwan, R.K.S., Pike, G.B., Evans, A.C.: Brainweb: Online interface to a 3D MRI simulated brain database. *NeuroImage* **5**, 425 (1997)
- Collignon, A., Vandermeulen, D., Suetens, P.: 3D multi-modality medical image registration using feature space clustering. In: 1th International Conference on Computer Vision, Virtual Reality and Robotics in Medicine, pp 193–204 (1995)
- Cornbleet, P.J., Gochman, N.: Incorrect least-squares regression coefficients in method-comparison analysis. *Clin. Chem.* **25**(3), 432–438 (1979)
- Goshtasby, A.A.: Image registration: principles, tools and methods. Springer (2012). <https://www.amazon.com/Image-Registration-Principles-Advances-Recognition-ebook/dp/B007ELLEE>
- Hazra, J., Roy Chowdhury, A., Dutta, P.: An approach for determining angle of rotation of a gray image using weighted statistical regression. *Int. J. Sci. Eng. Res.* **4**(8), 1006–1013 (2013)
- Hero, A.O., Ma, B., Michel, O.J.J., Gorman, J.: Applications of entropic spanning graphs. *IEEE Signal Process. Mag.* **19**(5), 85–95 (2002). <https://doi.org/10.1109/MSP.2002.1028355>
- Hill, D.L.G., Studholme, C., Hawkes, D.J.: Voxel similarity measures for automated image registration. *Vis. Biomed. Comput.* **2359**, 205–216 (1994)
- Liu, J., Meng, F., Mu, F., Zhang, Y.: An improved image retrieval method based on sift algorithm and saliency map. In: 2014 11th International Conference on Fuzzy Systems and Knowledge Discovery (FSKD), pp 766–770, (2014) <https://doi.org/10.1109/FSKD.2014.6980933>
- Lowe, D.G.: Distinctive image features from scale-invariant keypoints. *Int. J. Comput. Vis.* **60**(2), 91–110 (2004). <https://doi.org/10.1023/B:VISI.0000029664.99615.94>
- Ma, B., Hero, A.O., Gorman, J., Michel, O.: Image registration with minimal spanning tree algorithm. In: IEEE International Conference on Image Processing, pp 481–484 (2000)
- Maes, F., Vandermeulen, D., Suetens, P.: Medical image registration using mutual information. *Proc. IEEE* **91**, 1699–1722 (2003)
- Pál, D., Póczos, B., Szepesvári, C.: Estimation of Rényi entropy and mutual information based on generalized nearest-neighbor graphs. In: Proceedings of the 23rd International Conference on Neural Information Processing Systems - Volume 2, Curran Associates Inc., USA, NIPS'10, pp 1849–1857, (2010) <http://dl.acm.org/citation.cfm?id=2997046.2997102>. Accessed 30 Apr 2019
- Pluim, J.P.W., Maintz, J.B.A., Viergever, M.A.: Mutual-information-based registration of medical images: a survey. *IEEE Trans. Med. Imaging* **22**(8), 986–1004 (2003). <https://doi.org/10.1109/TMI.2003.815867>
- Póczos, B., Kirshner, S., Szepesvári, C.: REGO: Rank-based estimation of Rényi information using euclidean graph optimization. In: Teh, Y.W., Titterton, M. (eds.) Proceedings of the Thirteenth International Conference on Artificial Intelligence and Statistics, PMLR, Chia Laguna Resort, Sardinia, Italy, Proceedings of Machine Learning Research, vol 9, pp 605–612, <http://proceedings.mlr.press/v9/poczos10a.html> (2010). Accessed 30 Apr 2019
- Qin, B., Gu, Z., Sun, X., Lv, Y.: Registration of images with outliers using joint saliency map. *IEEE Signal Process. Lett.* **17**(1), 91–94 (2010). <https://doi.org/10.1109/LSP.2009.2033728>
- Redmond, C., Yukich, J.E.: Asymptotics for Euclidean functionals with power-weighted edges. *Stoch. Process. Appl.* **61**(2), 289–304 (1996). [https://doi.org/10.1016/0304-4149\(95\)00075-5](https://doi.org/10.1016/0304-4149(95)00075-5)
- Sabuncu, M.R., Ramadge, P.J.: Using spanning graphs for efficient image registration. *IEEE Trans. Image Process.* **17**(5), 788–797 (2008). <https://doi.org/10.1109/TIP.2008.918951>

20. Singh, S., Poczos, B.: Finite-sample analysis of fixed-k nearest neighbor density functional estimators. In: Lee, DD., Sugiyama, M., Luxburg, UV., Guyon, I., Garnett, R. (eds.) *Advances in Neural Information Processing Systems 29*, Curran Associates, Inc., pp 1217–1225, (2016) <http://papers.nips.cc/paper/6123-finite-sample-analysis-of-fixed-k-nearest-neighbor-density-functional-estimators.pdf>. Accessed 30 Apr 2019
21. Sricharan, K., Raich, R., Hero, A.O.: k-nearest neighbor estimation of entropies with confidence. In: *2011 IEEE International Symposium on Information Theory Proceedings*, IEEE, pp 1205–1209, (2011) <https://doi.org/10.1109/ISIT.2011.6033726>, <http://ieeexplore.ieee.org/document/6033726/>. Accessed 30 Apr 2019
22. Studholme, C., Hill, D.L.G., Hawkes, D.J.: An overlap invariant entropy measure of 3D medical image alignment. *Pattern Recognit.* **32**(1), 71–86 (1999). [https://doi.org/10.1016/S0031-3203\(98\)00091-0](https://doi.org/10.1016/S0031-3203(98)00091-0)
23. Viola, P., Wells III, W.M.: Alignment by maximization of mutual information. *Int. J. Comput. Vis.* **24**(2), 137–154 (1997). <https://doi.org/10.1109/ICCV.1995.466930>
24. Wachinger, C., Navab, N.: Entropy and laplacian images: Structural representations for multi-modal registration. *Med. Image Anal.* **16**(1), 1–17 (2012). <https://doi.org/10.1016/j.media.2011.03.001>
25. Woods, R.P., Mazziotta, J.C., Cherry, S.R.: MRI-PET registration with automated algorithm. *J. Comput. Assist. Tomogr.* **17**(4), 536–46 (1993). <https://doi.org/10.1097/00004728-199307000-00004>
26. Zhang, S., Zhi, L., Zhao, D., Zhao, H.: Minimum spanning tree hierarchically fusing multi-feature points and high-dimensional features for medical image registration. In: *2011 Sixth International Conference on Image and Graphics*, pp 263–266, (2011) <https://doi.org/10.1109/ICIG.2011.96>

Publisher's Note Springer Nature remains neutral with regard to jurisdictional claims in published maps and institutional affiliations.